

# Producing and measuring entanglement between two beams of microwave light

E. Flurin,<sup>1</sup> N. Roch,<sup>1</sup> F. Mallet,<sup>1</sup> M. H. Devoret,<sup>2,1,3</sup> and B. Huard<sup>1,\*</sup>

<sup>1</sup>Laboratoire Pierre Aigrain, Ecole Normale Supérieure,  
CNRS (UMR 8551), Université P. et M. Curie,

Université D. Diderot 24, rue Lhomond, 75231 Paris Cedex 05, France

<sup>2</sup>Collège de France, 11 Place Marcelin Berthelot, F-75231 Paris Cedex 05, France

<sup>3</sup>Department of Applied Physics, Yale University, PO Box 208284, New Haven, CT 06520-8284

(Dated: July 18, 2022)

**Pairs of entangled electromagnetic beams propagating on physically separated channels, the continuous variable version of Einstein-Podolsky-Rosen (EPR) states, constitute an essential resource in quantum information processing, communication and measurements. We have performed an interference experiment demonstrating the production and measurement of EPR states of microwave light using non-degenerate Josephson mixers. Driven by a pump tone, a first mixer generates a pair entangled beams out of vacuum quantum noise. A second mixer, driven by a phase shifted copy of the first pump tone, recombines and disentangles the two beams. We show that interference fringes of the intensity of the final output noise, referred to the input of the second mixer, pass under the level of vacuum for a range of phase shifts. The minimal measured noise intensity provides a quantitative measure of entanglement and yields a lower bound of 6 Mebits.s<sup>-1</sup> on the rate of entangled bits produced by the first mixer.**

At optical frequencies, Gaussian Einstein-Podolsky-Rosen (EPR) states [1, 2] are usually prepared by parametric down-conversion of a pump tone using a  $\chi^{(2)}$  non-linear medium [3]. EPR states can be viewed as a squeezed vacuum in the 4-dimensional phase space of the field quadratures  $\Re(a)$ ,  $\Im(a)$ ,  $\Re(b)$  and  $\Im(b)$  where  $a$  and  $b$  respectively are the field operators of the two beams, usually referred to as “signal” and “idler” [2]. The non-classical nature of the entanglement is revealed in the fluctuations of the combinations  $\Re(a) - \Re(b)$  and  $\Im(a) + \Im(b)$  at the output, which both fall below the level of quantum vacuum noise for a particular choice of phase reference. At microwave frequencies, only single-mode squeezing and squeezing of two sideband modes of a single transmission line have been demonstrated so far, using degenerate Josephson parametric amplifiers [4–8]. Recently, a dissipationless, non-degenerate, three-wave mixer for microwave signals based on Josephson junctions was developed [9–11]. Strong correlations between the spontaneously emitted radiations from two ports have been observed in the parametric down-conversion mode [12], but the experiment did not prove directly the presence of entanglement in the separated output beams. Here, we describe an interference experiment demonstrating that non-degenerate Josephson mixers can entangle and disentangle usable EPR states of microwave light. It consists of two such mixers placed back-to-back (Fig. 1). The first mixer, called the “entangler”, is driven by a pump tone while its two input ports are terminated by cold loads ensuring that only vacuum quantum noise enters the device. The two entangled output ports feed the input ports of the second mixer called the “analyzer”. The role of the analyzer is to disentangle the two microwave beams before sending them to a standard microwave amplification and detection chain. Interference fringes of the noise at the output of the analyzer, referred to its input, pass under the level of vacuum when the analyzer is in phase opposition with the entangler. Remarkably, the measurement of the noise at the output of the analyzer directly quantifies entanglement between its two input beams without resorting to two homodyne detection channels and the analysis of their correlation.

The Josephson dissipationless mixer [9–11] is a superconducting circuit parametrically coupling two superconducting resonators (Fig. 2) at distinct frequencies  $f_a$  and  $f_b$  via a pump at their sum frequency  $f_P = f_a + f_b$ . Each resonator has only one access port, but input and output signals are spatially separated by cryogenic microwave circulators (Fig. 2) so that the entangler output can be exclusively sent to the analyzer input. Each mixer performs a reversible transform of the wavefunction of the field via the unitary two-mode squeeze operator  $S = \exp(re^{i\varphi_P} a^\dagger b^\dagger - re^{-i\varphi_P} ab)$  where  $re^{i\varphi_P}$  is the complex squeezing parameter [13]. The input and output canonical field operators are related by the scattering relations

$$\begin{aligned} a_{out} &= S^\dagger a_{in} S = \cosh(r) a_{in} + e^{i\varphi_P} \sinh(r) b_{in}^\dagger \\ b_{out}^\dagger &= S^\dagger b_{in}^\dagger S = \cosh(r) b_{in}^\dagger + e^{-i\varphi_P} \sinh(r) a_{in} \end{aligned}$$

where  $\varphi_P$  is the phase of the pump and  $G = \cosh^2 r = (P_{th} + P)^2 / (P_{th} - P)^2$  is the power direct gain which increases with pump power  $P$  below the self parametric oscillation threshold  $P_{th}$ . With the pump on, the vacuum state at the

---

\*corresponding author: benjamin.huard@ens.fr

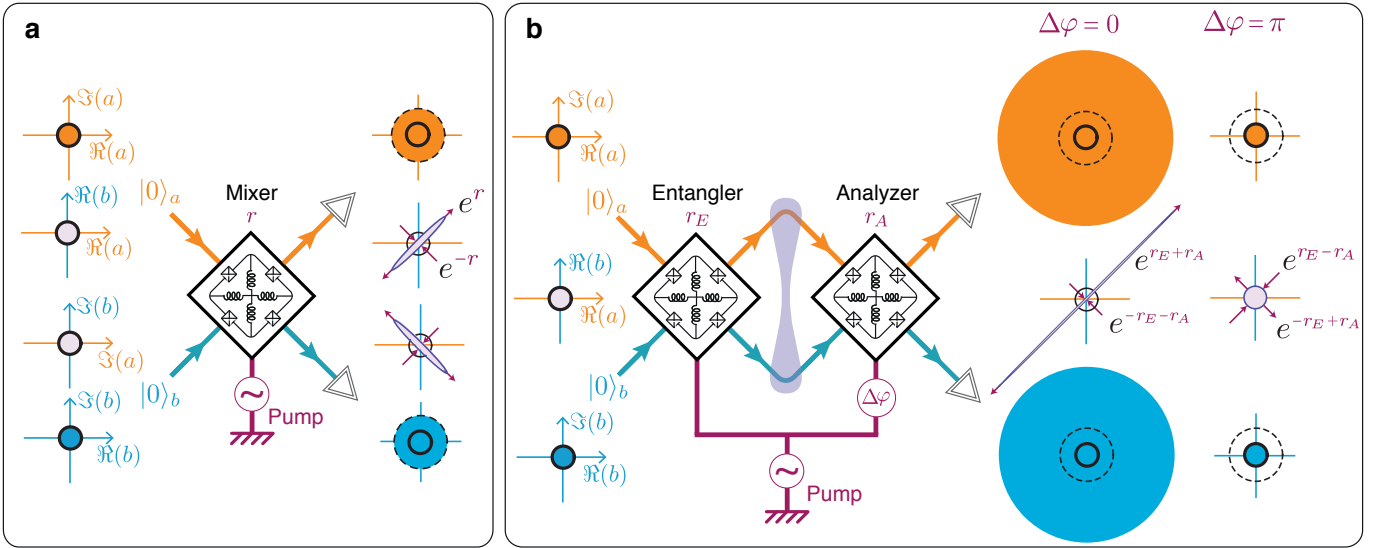


Figure 1: **Principle of the experiment.** **a.** When pumped with a microwave tone at frequency  $f_P = f_a + f_b$ , a Josephson non-degenerate mixer (black diamond) transforms incoming quantum vacuum noise on modes  $a$  and  $b$  into a two-mode squeezed state. The marginal distributions of the Wigner function of both modes can be represented as ellipses corresponding to standard deviation contours. The outcome of a measurement on individual modes can be determined in the quadrature phase space of modes  $a$  (top) and  $b$  (bottom). The correlations beyond quantum uncertainty are shown in the two-beam phase space spanned by  $(\Re(a), \Re(b))$  and  $(\Im(a), \Im(b))$  where  $\Re(a) = (a + a^\dagger)/2$  and  $\Im(a) = (a - a^\dagger)/2i$  are the in-phase and out-of phase quadratures of mode  $a$ . In each plot, a solid black circle sets the scale of vacuum noise and a dashed circle sets the size of the output noise with vacuum states at the input. The double-line triangle symbolizes a standard linear phase preserving amplifiers followed by a square law detector. **b.** Two mixers named “entangler” and “analyzer” are placed in series and pumped by two identical tones with phase difference  $\Delta\varphi$ . The entanglement between both beams is observed by measuring the intensity in each of the two output channels of the analyzer. This intensity presents interference fringes as the phase difference  $\Delta\varphi$  is varied. Here, we represent the noise ellipses for the maximum ( $\Delta\varphi = 0$ ) and minimum ( $\Delta\varphi = \pi$ ) of the fringes. Strikingly, at phase difference  $\Delta\varphi = \pi$  and coinciding squeezing parameters  $r_E = r_A$ , the analyzer reverses exactly the squeezing of the entangler back to the vacuum state. The analyzer output is therefore less noisy than for vacuum at its own input, which unambiguously demonstrates entanglement. Furthermore, the minimal measured noise is a direct measure of the quantity of entanglement between both beams at the input of the analyzer. The distributions are represented here for  $r_E = r_A = 1.2$ .

input is converted into a two-mode squeezed state  $|Sq\rangle = S|0\rangle_a|0\rangle_b$ . Note that this entangled state can be understood as the superposition of twin photons with different frequencies and propagating on spatially separated transmission lines. Two-mode squeezing directly appears in the non-local basis of maximally squeezed quadratures

$$a_{out} \pm e^{i\varphi_P} b_{out}^\dagger = e^{\pm r} \left( a_{in} \pm e^{i\varphi_P} b_{in}^\dagger \right) \quad (1)$$

which, for  $\varphi_P = 0$ , implies cross-correlations between  $\Re(a)$  and  $\Re(b)$  on one hand and  $\Im(a)$  and  $-\Im(b)$  on the other hand, beating the Heisenberg limit of vacuum quantum noise, as shown in Fig. 1. In optics, these correlations have been observed by double balanced homodyne detection techniques in several systems [14]. The present experiment describes the first demonstration at microwave frequencies of these quantum correlations between signals on spatially separated transmission lines. The Josephson mixer here serves two functions. First, it produces EPR states of microwave light on spatially and temporally non-degenerate modes similarly to optical parametric amplifiers [15]. Second, the two-mode squeeze operator  $S$  being reversible, the mixer is able to reverse the transformation and disentangle the field state. In the experiment, a first mixer called the entangler prepares a two-mode squeezed state with squeezing parameter  $r_E$  which is then processed by a second mixer called the analyzer with squeezing parameter  $r_A$  and relative pump phase  $\Delta\varphi$  (Fig. 1).

Very usefully, Josephson mixers have perfect transmission when not pumped. The output noise of the entangler can be measured on each mode independently by turning off the analyzer ( $r_A = 0$ ). The noise power spectrum measured by a spectrum analyzer is proportional to the symmetrized variance of the field operator [16]

$$(\Delta a_{out,E})^2 = \frac{1}{2} \left\langle \left\{ a_{out,E}, a_{out,E}^\dagger \right\} \right\rangle - | \langle a_{out,E} \rangle |^2 = \frac{1}{2} \cosh 2r_E. \quad (2)$$

This variance is always larger than that of the vacuum state, for which  $(\Delta a)^2 = 1/2$  (Fig. 1). Each output beam,

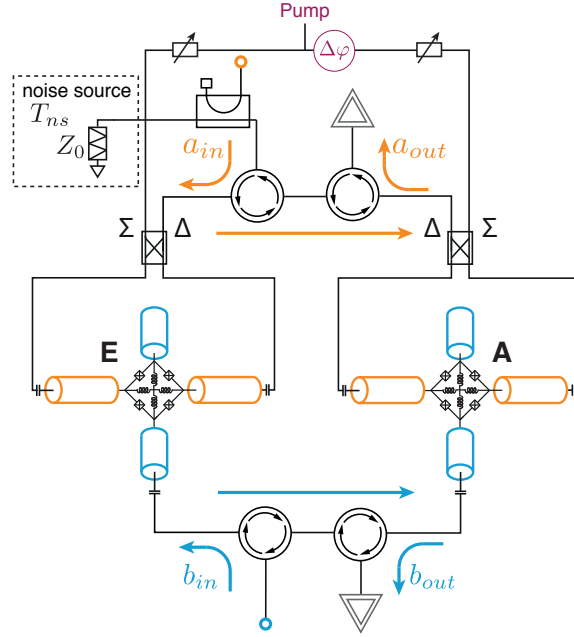


Figure 2: Schematics of the experimental setup. Each Josephson dissipationless mixer consists of a ring of Josephson junctions coupling two  $\lambda/2$  superconducting resonators addressed via  $180^\circ$  hybrid couplers. Both mixers are designed with the same geometry as in Ref. [11], and their matched resonance frequencies are  $f_a = 5.578$  GHz and  $f_b = 8.812$  GHz. The pump frequency is set to  $f_P = 14.390$  GHz. Microwave circulators separate the input and output of the entangler and analyzer. For calibration purposes [18], a load impedance with tunable temperature  $T_{ns}$  and thermally decoupled from the rest of the circuit at base temperature 45 mK is inserted at the  $a$  mode input of the entangler through a directional coupler. Unavoidable power losses  $\alpha$  and  $\beta$  have to be accounted for between both mixers in modes  $a$  and  $b$ . Each mixer can be tuned and calibrated separately by turning off the pump of the other one using the variable attenuators. Input ports are represented as open circles, and at each output port, a standard microwave measurement setup, represented as a double triangle, is made of a low noise amplifier based on high-electron-mobility transistors in series with additional amplifiers and a vector network analyzer or spectrum analyzer.

taken separately, is in a thermal state [17]. Yet, since the combined two-beam state  $|Sq\rangle$  is a pure state with no entropy, it is possible, in principle, to reverse the squeezing with a second mixer. One would re-obtain a vacuum state on each port which would demonstrate the presence of entanglement at the intermediate stage. Ideally, the analyzer can perform this inversion if operated with opposite squeezing parameter  $r_A = -r_E$ . In practice, unavoidable losses between the two mixers will spoil the recovery of the vacuum.

Losses are modeled as beam splitters coupling uncorrelated cold thermal baths to each mode (Fig. 3) so that

$$a_{in,A} = \sqrt{1 - \alpha} a_{out,E} + \sqrt{\alpha} a_{th} \text{ and } b_{in,A} = \sqrt{1 - \beta} b_{out,E} + \sqrt{\beta} b_{th} \quad (3)$$

where  $a_{th}$  and  $b_{th}$  describe bosonic modes of thermal baths at frequencies  $f_a$  and  $f_b$ . Besides, microwaves photons propagate for a finite amount of time  $\tau_a$  and  $\tau_b$  between the two mixers leading to a correction of the phase difference entering the scattering terms  $\Delta\varphi' = \Delta\varphi - 2\pi f_a \tau_a - 2\pi f_b \tau_b$ . The temporal extent of the twin photons exiting the entangler is given by the inverse of the bandwidth  $\Delta f = \Delta f_0 / \cosh r_E$  [12]. In the experiment, the travel times  $\tau_a$  and  $\tau_b$  of order 2 ns are much smaller than this temporal extent since  $\Delta f_0 = 28$  MHz, so that microwave photons do interfere even if their travel durations may slightly differ between modes. It is then straightforward to calculate the scattering coefficients of the full circuit. The  $a$  output mode is for instance given by

$$a_{out,A} = t_{a \rightarrow a} a_{in,E} + t_{b \rightarrow a} b_{in,E}^\dagger + \sqrt{\alpha} \cosh r_A a_{th} + e^{i\Delta\varphi} \sqrt{\beta} \sinh r_A b_{th}^\dagger. \quad (4)$$

where

$$\begin{cases} t_{a \rightarrow a} = \sqrt{1 - \alpha} \cosh r_E \cosh r_A + e^{i\Delta\varphi} \sqrt{1 - \beta} \sinh r_E \sinh r_A \\ t_{b \rightarrow a} = \sqrt{1 - \alpha} \sinh r_E \cosh r_A + e^{i\Delta\varphi} \sqrt{1 - \beta} \cosh r_E \sinh r_A \end{cases}. \quad (5)$$

The scattering coefficients of Eq. (5) were measured using a non-linear four-port vector network analyzer for a whole set of parameters  $r_E$  and  $r_A$ . The transmission coefficients have been measured as a function of the phase

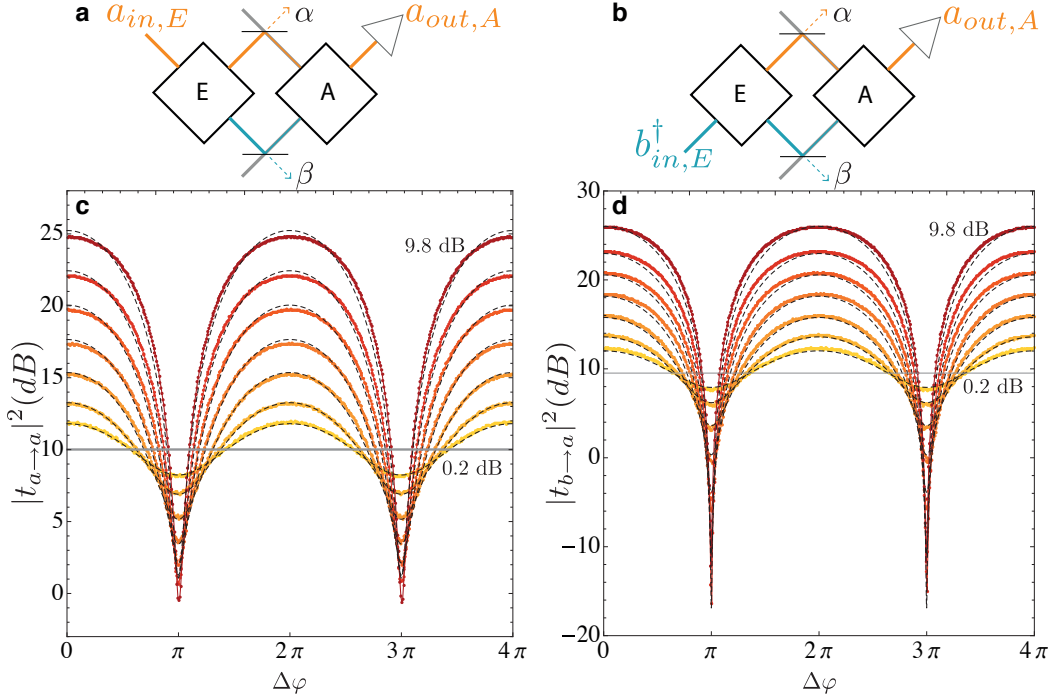


Figure 3: **a,b.** Protocol of the scattering coefficient measurements by a vector network analyzer connected between the  $a$  or  $b$  input port and the  $a$  output port. The setup is calibrated by turning on and off each Josephson mixer separately. Losses are modeled as beam splitters of transparency  $\alpha^2$  and  $\beta^2$  coupling a cold load to the signals. **c.** Color traces: Transmission measurements of  $|t_{a \rightarrow a}|^2$  as a function of phase difference  $\Delta\varphi$  between both pump signals. The gain of the analyzer is set to  $G_A = \cosh^2 r_A = 10$  (solid gray line). Each trace and color corresponds to a different gain for the entangler  $G_E = \cosh^2 r_E = 0.2, 0.8, 1.8, 3.2, 5, 7.2, 9.8$  dB. Dashed lines: fits to the data using equation (5) and the single fit parameter  $(1 - \beta)/(1 - \alpha) = 0.945$ . **d.** Same measurement as in panel 3c, but between input mode  $a_{in,E}$  and output mode  $b_{out,A}$  (frequency conversion measurement).

difference  $\Delta\varphi$  for various values of the gains  $\cosh^2 r_{E,A}$  ranging from 1 to 40, a subset of which is shown on Fig. 3. The special cases where one or both of the converters are not pumped ( $r = 0$ ) offer the opportunity to calibrate each converter gain independently. The only fit parameter for this whole set of measurements is the ratio between transmissions on both arms, found to be  $(1 - \beta)/(1 - \alpha) = 0.945$ .

In Fig. 3, only mean values of the output field amplitudes are measured. Yet, truly quantum features appear in their correlations. Consider the case of a cold load setting the vacuum quantum state at the input of the entangler, which is reached in our experiment at 45 mK since  $hf_b/k > hf_a/k = 260$  mK [18]. When the entangler is turned off ( $r_E = 0$ ), the analyzer is fed by vacuum fluctuations and the output noise reads  $(\Delta a_{out,A})^2 = \cosh(2r_A)/2$  as in Eq. (2). In general, the output noise  $\sigma^2$ , normalized to that reference level, on both output ports can be calculated from Eq. (5) and oscillates with phase  $\Delta\varphi$  as

$$\sigma^2(\Delta\varphi) \equiv \frac{2(\Delta a_{out,A})^2}{\cosh(2r_A)} = (1 - \alpha) (\cosh 2r_E + \sinh 2r_E \tanh 2r_A \cos \Delta\varphi) + \alpha. \quad (6)$$

For simplicity, this expression is only given in the case of balanced losses  $\alpha = \beta$ , but the general case can be treated without much difficulty. It is worthwhile to note that the resulting interference fringes are obtained using an input signal which does not have a defined phase: the vacuum state. The maximal and minimal values of the noise, obtained respectively for  $\Delta\varphi = 0$  and  $\Delta\varphi = \pi$ , read

$$\sigma_{\max,\min}^2 = (1 - \alpha) \frac{\cosh(2r_E \pm 2r_A)}{\cosh(2r_A)} + \alpha. \quad (7)$$

This variance is equal to that of a vacuum state  $\sigma_{|0\rangle}^2 = \cosh^{-1}(2r_A)$  (or  $(\Delta a)^2 = 1/2$ ) only for opposite complex squeezing parameters on both mixers  $r_A = -r_E$  and zero loss  $\alpha = 0$ . Under these conditions, the intermediate state  $|Sq\rangle$  is exactly unsqueezed back to the vacuum. In practice, finite losses forbid this exact unsqueezing but the

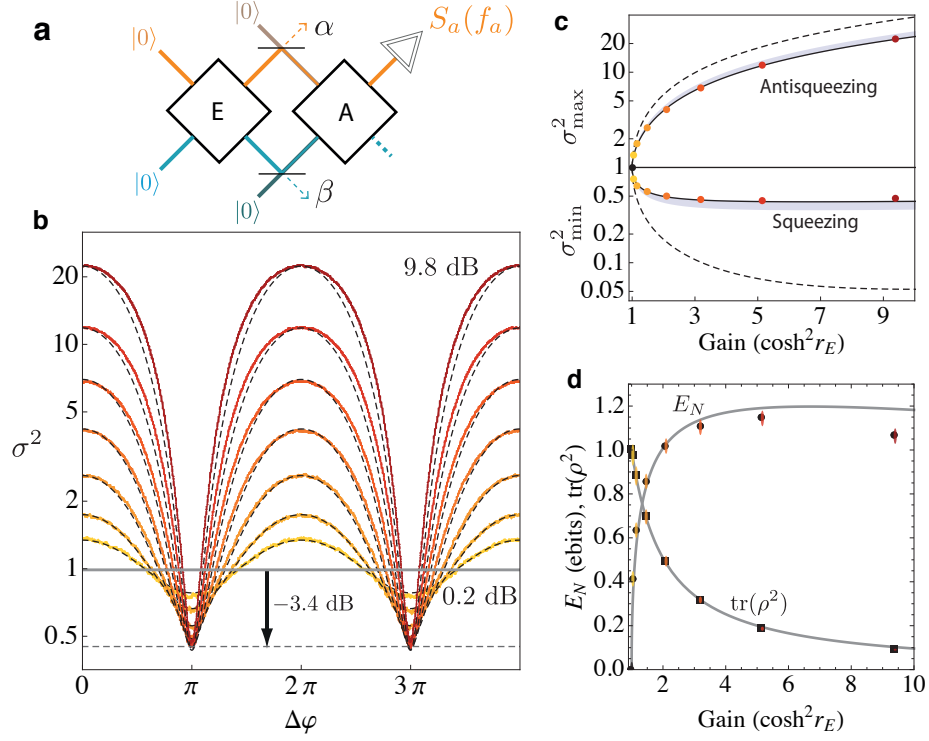


Figure 4: **a.** Protocol of the experiment with losses  $\alpha$  and  $\beta$  between mixers. An independent, *in situ* calibration gives  $\alpha = 0.33 \pm 0.05$  and  $\beta = 0.36 \pm 0.05$  [18]. **b.** Color traces: variance of the output mode  $(\Delta a_{outA})^2$  referred to the case of vacuum input on the analyzer (divided by  $\cosh(2r_A)/2$ ) as a function of phase difference  $\Delta\varphi$  determined by measuring the spectral density of the noise outputting mode  $a$ . An absolute calibration of the spectral density using a thermal noise source allowed exact conversion between both quantities with an error of at most  $\pm 2.5\%$  [18]. Each curve and color corresponds to a different gain of the entangler  $G_E = \cosh^2 r_E = 0.2, 0.8, 1.8, 3.2, 5, 7.2, 9.8$  dB with a fixed gain on the analyzer  $G_A = \cosh^2 r_A = 10$ . The horizontal line represents the measured noise with vacuum fluctuations at the input of the analyzer ( $r_E = 0$ ). For  $\Delta\varphi \approx \pi$ , the measured noise goes below this level, an evidence of entanglement. Dashed lines: predicted variance using Eq. (6) extended to the unbalanced loss case using  $\alpha = 0.37$  and  $\beta = 0.40$ . **c.** Dots: Noise level measured at  $\Delta\varphi = 0$  (anti-squeezing) and  $\Delta\varphi = \pi$  (squeezing) as a function of gain  $G_E$  for  $G_A = 10$ . The size of the points is larger than the error bar. Solid lines: prediction using Eq. (7), extended to unbalanced losses as in panel 4b. Colored area: consistent values of the noise using the uncertainty in the calibration of the losses  $\alpha$  and  $\beta$  [18]. Dashed lines: same prediction but without losses,  $\alpha = \beta = 0$ . **d.** Disks: the  $\log_2$  of the minima from panel 4c lead to a quantification of the entanglement called the logarithmic negativity. The disks plot this quantity and the colored ellipses are the error bars. Squares: using the same data, one quantifies the purity  $\text{tr}(\rho^2)$  of the entangled beams. Lines: logarithmic negativity and purity of the state at the input of the analyzer as a function of  $r_E$  using the same parameters as in the solid lines of panel 4c (see text).

analyzer can still measure accurately the entanglement at its input. Indeed, the existence of a phase  $\Delta\varphi$  for which the output noise  $\sigma^2$  goes below 1, which is the level of vacuum input on the analyzer, is a sufficient evidence of entanglement (see Methods). It is remarkable that the amount of noise at the output of a single port of the analyzer directly measures the entanglement between the two input beams. In particular, the minimum of output noise is directly linked to the logarithmic negativity  $E_N = -\log_2(\sigma_{\min}^2)$  and the entropy of formation  $E_F$  (see Methods): the deeper the noise fringes, the larger the entanglement. The purity of the entangled state is also directly related to both extrema  $\text{tr}(\rho^2) = (\sigma_{\min}^2 \sigma_{\max}^2)^{-1}$ .

The spectral densities  $S_a(f_a)$  and  $S_b(f_b)$  of both modes at the output of the analyzer were measured using a microwave spectrum analyzer behind a cryogenic low-noise preamplifier on a 0.5 MHz bandwidth. This bandwidth was chosen to be smaller than that of the mixers for all combinations of gains  $G_{E,A} = \cosh^2 r_{E,A}$  and phase differences  $\Delta\varphi$ . For large enough gains of the analyzer, the contribution to the noise due to the following amplifiers is small enough to subtract it precisely. Importantly, it was possible to calibrate the normalized noise power at the output of the analyzer from the measured spectral densities with at most  $\pm 2.5\%$  relative error [18]. This calibration was performed by turning on a single mixer at a time and varying the temperature  $T_{\text{ns}}$  of a thermally decoupled input load on mode  $a_{in,E}$  [18]. As a side result, the calibration provides the loss  $\alpha = 0.33 \pm 0.05$  between mixers on mode  $a$  which, together with the ratio  $(1 - \beta)/(1 - \alpha) = 0.945$  from Fig. 3, leaves no unknown parameters in the experiment.

The measured noise powers hence directly give  $\sigma^2$  as a function of phase difference  $\Delta\varphi$ . As can be seen on Fig. 4b, the noise does pass below the threshold of amplified vacuum noise, hence proving the existence of entanglement. Note that minimum noise  $\sigma_{\min}^2$  does not occur for opposite squeezing parameters since it increases again at large gains. This deviation may be due to the beginning of a saturation of the analyzer mixer, corroborated by the slight deviations in Fig. 3. For each squeezing parameter  $r_E$ , it is possible to extract the extrema of noise  $\sigma_{\min,\max}^2$  from the curves of Fig. 4b. These extremal noise measurements (Fig. 4c) are well described by Eq. (7) generalized to unbalanced losses between modes with  $\alpha = 0.37$  and  $\beta = 0.40$ , consistently with the calibration. It is even possible to account for the whole dependence of the measured noise on phase difference  $\Delta\varphi$  by generalizing Eq. (6) using the same parameters (Fig. 4b). The overall minimum for the measured noise is reached at  $r_E \approx 1.5$  and reads  $\sigma_{\min}^2 = 0.45 \pm 0.01$  with a corresponding maximum  $\sigma_{\max}^2 = 11.9 \pm 0.1$ . These values directly lead to a logarithmic negativity  $E_N = -\log_2(\sigma_{\min}^2) = 1.15 \pm 0.04$ , a purity  $\text{tr}(\rho^2) = 0.186 \pm 0.09$  and an entropy of formation  $E_F = 0.69 \pm 0.03$  entangled bits (ebits, see Methods). These quantities of entanglement are not far from the state of the art in optics [19–22]. Given the bandwidth of the mixers at  $r_E = r_A = 1.8$ , the analyzer receives a usable rate of 6 Mebits.s<sup>-1</sup> from the entangler.

In conclusion, the production of entangled beams of microwave radiation by a Josephson mixer has been demonstrated by a quantum noise interference experiment. Vacuum noise at the input of a first mixer is converted into two entangled beams. A second mixer is used to disentangle the two beams. Using an absolute calibration, the minimal noise intensity at the output of the second mixer, when the phase difference  $\Delta\varphi$  is varied, constitutes a direct measure of the entanglement between the twin beams. Our measurements are limited by the finite losses between mixers but still show that a rate of 6Mebits.s<sup>-1</sup> travel between the entangler and the analyzer. This first implementation of EPR Gaussian states in the microwave domain opens novel opportunities for quantum teleportation or superdense coding in the fields of nanomechanical resonators and superconducting qubits. In particular, inserting a "circuit QED" readout cavity in one arm of the vacuum quantum noise interferometer described in this paper, one would achieve a maximally efficient measurement, for a given photon number, of the phase shift associated with a change of qubit state.

**Methods.** In the phase-space mapped by  $\vec{x} = (\Re(a), \Im(a), \Re(b), \Im(b))^T$ , the mixer performs a transformation described by

$$S(r, \varphi) = \begin{pmatrix} \cosh(r)\mathbb{I}_2 & \sinh(r)\mathbf{Z}\mathbf{R}(\varphi) \\ \sinh(r)\mathbf{Z}\mathbf{R}(\varphi) & \cosh(r)\mathbb{I}_2 \end{pmatrix} \quad (8)$$

where

$$\mathbb{I}_2 = \begin{pmatrix} 1 & 0 \\ 0 & 1 \end{pmatrix}, \mathbf{Z} = \begin{pmatrix} 1 & 0 \\ 0 & -1 \end{pmatrix} \text{ and } \mathbf{R}(\varphi) = \begin{pmatrix} \cos \varphi & \sin \varphi \\ -\sin \varphi & \cos \varphi \end{pmatrix}. \quad (9)$$

The covariance matrix  $\mathbf{V}$  is defined by its elements  $\mathbf{V}_{ij} = \frac{1}{2} \langle \{x_i - \langle x_i \rangle, x_j - \langle x_j \rangle\} \rangle$  where  $\{.,.\}$  denotes the anti-commutator and  $x_i$  is the  $i$ -th component of  $\vec{x}$  [2]. Assuming a Gaussian state symmetric between  $a$  and  $b$  modes at the input of the analyzer, and by choosing the phase reference appropriately, the covariance matrix of the state at the input of the analyzer can be written as

$$\mathbf{V}_{in,A} = \begin{pmatrix} n & 0 & k & 0 \\ 0 & n & 0 & -k \\ k & 0 & n & 0 \\ 0 & -k & 0 & n \end{pmatrix}. \quad (10)$$

Two beams at the input of the analyzer are entangled iff  $\delta \equiv 4(n-k) < 1$  [23]. For unpure states, multiple, inequivalent measures of entanglement coexist [24]. The logarithmic negativity  $E_N$ , an upper bound to the distillable entanglement, quantifies how negative are the eigenvalues of the partially transposed density matrix. It is directly related to  $\delta$  via  $E_N = -\log_2 \delta$  [25, 26]. Introducing  $\Sigma = 4(n+k)$ , it is straightforward to calculate the purity of the entangled state  $\mu = \text{tr}(\rho^2) = (\det \mathbf{V}_{out,A})^{-1/2} = (\Sigma\delta)^{-1}$  [20]. In the case of Gaussian states, one of the most intuitive measure is the entropy of formation  $E_F$ . For a given density matrix  $\rho$  describing the state shared by two distant observers Alice and Bob,  $E_F(\rho)$  corresponds to the number of EPR singlets they need to share in order to reconstruct  $\rho$  with classical communications only [27]. For a pure state whose Schmidt decomposition reads  $\sum_n c_n |a_n\rangle |b_n\rangle$ , the entropy of formation is  $E_F = -\sum_n c_n^2 \log_2(c_n^2)$ . For the Gaussian pair of beams at the input of the analyzer, the calculation can be extended and gives [23, 28]

$$E_F(n, k) = c_+ \log_2(c_+) - c_- \log_2(c_-) \quad (11)$$

where  $c_{\pm} = (\delta^{-1/2} \pm \delta^{1/2})^2 / 4$ . Note that the entropy of formation is a decreasing function of  $\delta$ .

Besides, the covariance matrix at the output of the analyzer is  $\mathbf{V}_{out,A} = S(r_A, \Delta\varphi)\mathbf{V}_{in,A}S(r_A, \Delta\varphi)^T$ . A simple spectrum analyzer at the output of mode  $a$ , such as in Fig. 4, measures the sum of the two first diagonal terms of the covariance matrix  $S_a(f_a) \propto (\Delta a_{out,A})^2 = \mathbf{V}_{out,A,11} + \mathbf{V}_{out,A,22}$ . Therefore, one gets  $S_a(f_a) \propto n \cosh(2r_A) + k \sinh(2r_A) \cos \Delta\varphi$ . Using the absolute calibration described in [18], we normalize the measured spectral density to 1 for a vacuum state at the input of the analyzer ( $n = 1/4, k = 0$ ) so that, in these normalized units

$$\sigma^2(\Delta\varphi) = 4(n + k \tanh(2r_A) \cos \Delta\varphi). \quad (12)$$

In the limit of large squeezing parameter  $r_A$ , such as in the experiment of Fig. 4, the minimal measured noise  $\sigma_{\min}^2$  as a function of phase difference  $\Delta\varphi$  is equal to  $\delta$ . The smaller the minimum noise, the higher the entanglement between input beams of the analyzer. In the experiment, for  $r_E = 1.5$  and  $G_A = 10$ , the noise goes as low as  $\delta \approx 4[n - k \tanh(2r_A)] = 0.45 \pm 0.01$  for  $\varphi \approx \pi$ , which leads to a logarithmic negativity  $E_N = -\log_2 \delta = 1.15 \pm 0.04$ . The entropy of formation is given by Eq. (11), leading to  $E_F = 0.69 \pm 0.03$  entangled bits (ebits) at the input of the analyzer. Note that without any loss between the entangler and the analyzer [18], we should have measured  $\delta = e^{-2r_E}/4$ , which corresponds to  $E_F = 4.6$  ebits at the output of the entangler for the same squeezing parameter  $r_E = 1.8$ . Finally, using the maximal measured noise  $4(n+k) \approx \sigma_{\max}^2 = 11.9 \pm 0.01$ , one gets the purity of the entangled state  $\mu = \text{tr}(\rho^2) = 0.186 \pm 0.09$  at  $r_E = 1.5$  [20].

- 
- [1] S. Braunstein and P. van Loock, *Rev. Mod. Phys.* **77**, 513 (2005).
  - [2] C. Weedbrook et al., arXiv 1110.3234v1 (2012) to be published in *Rev. Mod. Phys.*
  - [3] R. Slusher, L. Hollberg, B. Yurke, J. Mertz, and J. Valley, *Phys. Rev. Lett.* **55**, 2409 (1985).
  - [4] B. Yurke, et al., *Phys. Rev. Lett.* **60**, 764 (1988).
  - [5] M. A. Castellanos-Beltran, K. D. Irwin, L. R. Vale, G. C. Hilton, and K. W. Lehnert, *Nature Phys.* **4** 929 (2009).
  - [6] F. Mallet et al., *Phys. Rev. Lett.* **106**, 220502 (2011).
  - [7] C. Eichler et al., *Phys. Rev. Lett.* **107**, 113601 (2011).
  - [8] C.M. Wilson et al., *Nature (London)* **479**, 376 (2011).
  - [9] N. Bergeal et al., *Nature Phys.* **6**, 296 (2010).
  - [10] N. Bergeal et al., *Nature (London)* **465**, 64 (2010).
  - [11] N. Roch et al., arXiv 1202.1315v1 (2012) to be published in *Phys. Rev. Lett.*
  - [12] N. Bergeal, F. Schackert, L. Frunzio, and M. H. Devoret, arXiv 1011.4000 (2012) to be published in *Phys. Rev. Lett.*
  - [13] G. Grynberg, A. Aspect, and C. Fabre, *Introduction to Quantum Optics*, Cambridge University Press (2010).
  - [14] M. D. Reid et al., *Rev. Mod. Phys.* **81**, 1727 (2009).
  - [15] J. Wenger, A. Ourjoumtsev, R. Tualle-Brouiri, and P. Grangier, *Eur. Phys. J. D* **32**, 391 (2005).
  - [16] A. Clerk, M. Devoret, S. Girvin, F. Marquardt, and R. Schoelkopf, *Rev. Mod. Phys.* **82**, 1155 (2010).
  - [17] P. D. Drummond and Z. Ficek, *Quantum Squeezing* (Berlin, Heidelberg, New York, Springer-Verlag) (2004).
  - [18] Supplementary Information.
  - [19] J. Laurat, T. Coudreau, G. Keller, N. Treps, and C. Fabre, *Phys. Rev. A* **71**, 022313 (2005).
  - [20] J. DiGuglielmo, B. Hage, A. Franzen, J. Fiurášek, and R. Schnabel, *Phys. Rev. A* **76**, 012323 (2007).
  - [21] Y. Takeno, M. Yukawa, H. Yonezawa, and A. Furusawa, *Optics Express* **15**, 4321 (2007).
  - [22] T. Eberle et al., *Phys. Rev. A* **83**, 052329 (2011).
  - [23] G. Giedke, M. Wolf, O. Krüger, R. Werner, and J. Cirac, *Phys. Rev. Lett.* **91**, 107901 (2003).
  - [24] R. Horodecki, M. Horodecki, and K. Horodecki, *Rev. Mod. Phys.* **81**, 865 (2009).
  - [25] G. Vidal and R.F. Werner, *Phys. Rev. A* **65**, 032314 (2002).
  - [26] G. Adesso and F. Illuminati, *Phys. Rev. A* **72**, 032334 (2005).
  - [27] C. Bennett, D. DiVincenzo, J. Smolin, and W. Wootters, *Phys. Rev. A* **54**, 3824 (1996).
  - [28] P. Marian and T. Marian, *Phys. Rev. Lett.* **101**, 220403 (2008).

**Acknowledgments.** We are grateful to N. Treps, T. Kontos and J.-P. Poizat for fruitful discussions, P. Morfin for technical assistance and P. Pari for giving us RuO<sub>2</sub> thermometers. Nanofabrication has been made within the consortium Salle Blanche Paris Centre. This work was supported by the EMERGENCES program Contract of Ville de Paris and by the ANR contract ULAMSIG.

**Author contributions** E.F. fabricated the mixers. E.F. and N.R. carried out the measurements. All authors contributed to the design of the experiment, its interpretation and to the manuscript.